PERGAMON

International Journal of Heat and Mass Transfer 42 (1999) 1007–1022

International Journal of HEAT and MASS TRANSFER

Heat transfer from a horizontal wafer-based disk of multi-chip modules

Y. R. Shieh[1], C. J. Li[1], Y. H. Hung*[,2]

Department of Power Mechanical Engineering, National Tsing Hua University, Hsinchu 30043, Taiwan

Received 3 January 1998; in final form 21 May 1998

Abstract

Convective heat transfer characteristics above a horizontal wafer-based disk heated with 15 simulated chips in unobstructed ambient air have been experimentally investigated under both stationary and rotating disk conditions. Relevant parameters influencing heat transfer performance studied are the Grashof number and rotational Reynolds number. Their effects on heat transfer characteristics in such configurations of stationary and rotational heated disks are successively explored. The heat transfer enhancement of rotation on the heated disk has been investigated; the effect of natural convection on the heat transfer behavior of the heated rotating disk has also been explored. Three heat transfer regimes dominated by purely forced convection of rotation, mixed convection and purely natural convection are classified over a wide range of a system parameter, Gr/Re_r^2. Also, in the natural convection aspect, two new empirical correlations of average Nusselt number in terms of temperature difference and Grashof number are proposed. In the mixed convection aspect, another two explicit composite correlations of average Nusselt number for mixed convection caused by the mutual effect of disk rotation and buoyancy are also proposed. Satisfactory comparisons of the predictions evaluated by the proposed correlations with the present experimental data are achieved.

Nomenclature

D diameter of the wafer-based disk
D_h hydraulic diameter of simulated chips, $2\ell w/(\ell + w)$
Gr Grashof number, $\beta g \overline{\Delta T} D^3/\nu^2$
h heat transfer coefficient
k_f thermal conductivity of air
ℓ simulated chip length
N rotational speed of the disk in rpm
$\underline{Nu_i}$ Nusselt number of chip i, $h_i D_h/k_f$
$\overline{Nu}$ average disk Nusselt number, $\bar{h}D/k_f$
Pr Prandtl number, ν/α
q heat flux
Re_r rotational Reynolds number, $\pi N D^2/120\nu$
T temperature
w simulated chip width.

Greek symbols
α thermal diffusivity of air
ε emissivity of disk surface
η kinematic viscosity of air
Ω electric resistance
ρ density of air.

Superscript
$^-$ average.

Subscripts
a ambient
c convection
i simulated chip number
k conduction
r radiation or rotation
t total
w surface.

1. Introduction

The design of cooling for systems in rotation, such as high-power electronics packaging, high-duty computer

* Corresponding author. Tel.: +886-3-5712312; Fax: +886-3-5722840; E-mail: yhhung@pme.nthu.edu.tw
[1] Graduate student
[2] Professor

0017–9310/98/$—see front matter
PII: S0017–9310(98)00182–3

aided tomography (CAT) scanners, rotational trays of chemical vapor deposition (CVD) systems, turbines and electric motors, as well as the design of rotating heat exchangers, high-speed gas bearings, and a variety of other equipment, requires an understanding of convective heat transfer with rotation. Therefore, the heat transfer characteristic of rotation is not only of theoretical interest, but also of great practical importance. For example, as we know, a traditional passive cooling technique such as the natural convection method is no longer adequate for the anticipated high heat flux of modern electronics packaging. Based on the survey presented by Bergles [1], a mechanical aid with surface rotation is one of the most effective methods for cooling augmentation.

The rotating circular disk is one of a number of geometrical configurations of interest because many practical systems can be idealized as a circular disk rotating in an open environment or in a limited-space housing. Therefore, the flow and heat transfer characteristics in the three-dimensional boundary layer over a rotating circular disk have been studied extensively in the past. Most of the existing literature was limited to forced convection situations where forces and momentum transport rates are large enough so that natural convection effects can be ignored. Nevertheless, in many practical circumstances of small/moderate flow velocities or large wall-fluid temperature differences, the influences of buoyancy forces and associated natural convection motions may significantly affect both the flow and heat transfer characteristics. Therefore, the motivation of the present study is to experimentally explore the mutual effect between rotation and buoyancy on the heat transfer behavior of a wafer-based rotating disk having 15 simulated heated chips in unobstructed ambient air; and then to evaluate the feasibility of using the method of rotation on the applications of multi-chip modules (MCMs) cooling.

Natural convection heat transfer from a finite-size, horizontal heated disk is complicated by the interaction of entrained flow along the disk with the separated flow from the heated surface. Two important parameters influencing the flow structure are the geometry and a properly defined Grashof number. Limits can be identified as (1) a point heat source which releases thermal energy in the form of an axisymmetric plume, and (2) a large horizontal disk which, in the limit, neglects the radial geometry over a large portion of the disk and assumes that the central region, where flow separation occurs, is of minor importance to the heat transfer. The above-mentioned limits have been analytically and numerically solved [2–4].

Experiments on natural convection adjacent to horizontal plane surfaces were performed by Goldstein et al. [5] using the naphthalene sublimation technique. Then, by analogy, the mass transfer results were analogous to heat transfer aspects. In 1983, Goldstein and Lau [6] extended their results by finite difference solutions and mass transfer experiments to consider the influence of plate-edge extensions with six geometries. In addition, Al-Arabi and El-Riedy [7] carried out a series of experiments on natural convection heat transfer from isothermal plates with different shapes (square, rectangular and circular) in the range of $GrPr$ from 2×10^5–10^9. In 1984, Ellison [8] conducted several natural convection experiments in air for the purpose of thermal control of electronic equipment and proposed two empirical formulas. Also in Ref. [9], empirical correlations for uniform wall temperature and uniform wall heat flux had been collected in Ozisik and Bayazitoglu's heat transfer book. Recently, in our laboratory, Huang [10] conducted a series of natural convection in the range of Grashof number from 1.248×10^6–2.353×10^6 to examine the effect of natural convection in jet impingement study.

As for the rotating disk, the hydrodynamic phenomena in an infinite environment were investigated theoretically by von Karman [11]. Based on these flow conditions, the coefficient of heat transfer from a rotating disk to ambient air in case of a laminar boundary layer was theoretically calculated by Wanger [12]. Hartnett [13] extended the research to consider the influence of a variation in the surface temperature on the heat transfer from a disk rotating in still air, allowing the temperature difference between the disk surface and the fluid at rest to vary as a power function of the radius. Then, the restriction of Prandtl number was lifted by Sparrow and Gregg [14] and Riley [15]. Experimentally measured mass transfer rates from a disk rotating in an infinite environment under laminar and turbulent conditions were conducted by Kreith et al. [16] and the results were related to the corresponding heat transfer process by means of an analogy method. In 1960, Tien [17] indicated that the heat transfer results for a rotating disk can also be used for a rotating cone under boundary layer approximations. Screenivasan [18], by assuming the flow was steady, laminar, incompressible, and non-dissipative, investigated the effect of buoyancy on the flow and heat transfer above a heated, horizontal, rotating disc. The local heat transfer coefficients were reported experimentally over an isothermal disk surface rotating in still air by Popiel and Boguslawski [19]. In 1979, Oehlbeck and Erian [20], assuming that natural convection and viscous dissipation effects were both negligible, examined the effect of radial distribution of temperature or heat flux, and showed the effects of Prandtl number, Reynolds number, and radial conduction on heat transfer coefficients from various heater source geometries. A new similarity variable was proposed by Lin and Lin [21] for the analysis of laminar boundary layer heat transfer from a rotating cone or disk to fluids of any Prandtl number.

According to the literature survey [22], although there were many attempts to explore natural convection from a horizontal heated disk and heat transfer characteristics of a rotating disk in unobstructed fluid, most of them

were studied using analytical or numerical methods. The existing experimental data were still very scarce. Besides, their attention was mostly focused on average Nusselt number. Furthermore, the mutual effect of rotation and buoyancy on heat transfer behavior of a rotating disk having discrete heating sources was seldom considered. In order to advance our understanding on heat transfer characteristics of a rotating circular wafer-based disk having 15 simulated heating chips in unobstructed ambient air, a series of systematic experiments have been performed. The objectives of this research include (1) to investigate the natural convection behavior on a horizontal stationary wafer-based disk having 15 simulated heating chips; (2) to examine the effect of rotation on heat transfer enhancement of such a horizontal heated disk; (3) to compare the present experimental results with existing data; (4) to classify heat transfer regimes for a horizontal heated disk having a mutual effect caused by disk rotation and buoyancy; (5) to propose new composite correlations of average Nusselt numbers over a wide range of system parameters, Gr and Re_r; and (6) to evaluate the feasibility of using active method of rotation on the cooling of a wafer-based disk of MCMs.

2. The experiments

Figure 1 shows the overall experimental setup with the relevant apparatus and instruments. The present experimental facilities are composed of three major parts, i.e., (1) rotating facility, (2) test block, and (3) apparatus and instrumentation. Brief descriptions for general configurations and functions of the facilities are introduced in the following.

2.1. Rotating facility

The system platform is shown in Fig. 2. The heated assembly of wafer-based disk can be directly mounted on

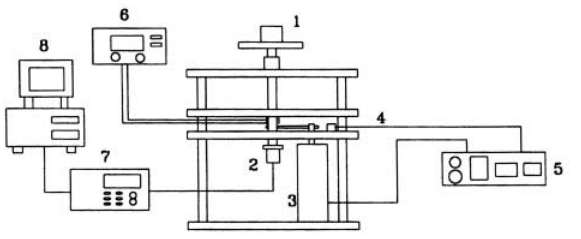

Fig. 1. Overall experimental setup for a MCM disk in unobstructed ambient air.

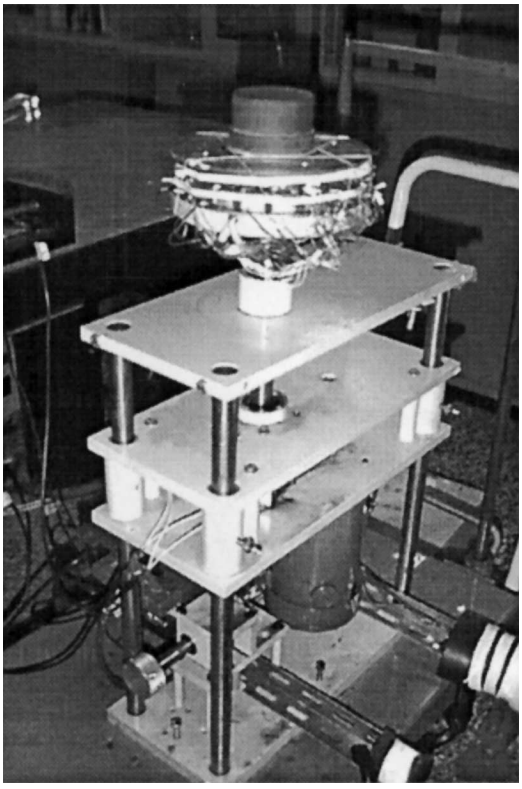

Fig. 2. Rotating facility in the experiment.

the spindle of the platform to rotate freely in unobstructed ambient air. The spindle is driven by an 0.5 hp d.c. motor. Furthermore, the heated disk assembly is able to move in vertical direction to control the separation distance driven by a step motor. The body of platform is a 3-level structure supported by four posts standing at its four corners. The upper and lower levels are end plates to hold the four posts in position. The altitude of the center level where a rotational mandrel is attached is controllable to give the desired position of the rotational disk. Limiting switches are equipped to protect the movement of the center level from collision with other components. There is a 20-channel slip ring located at the lower end of the rotational mandrel to transfer the signal from thermocouples to the data logger. All the thermocouples from the test block through the rotational mandrel are connected to the rotational slide of slip ring which is rotating with the rotational mandrel. The respective 20 channels on the other end, the stationary side of slip ring, is fixed to the center level of the platform and connected to the Fluke NetDAQ 2640A data logger. The rotation velocity can be controlled by the control box by the signal feedback of a tachometer.

2.2. Test block

The test block has a diameter of 80 and 85 mm thick. The block, which is confined with bakelite, is composed of three layers. As shown in Fig. 3, the top layer is the wafer-based disk of simulated MCM, which is made by a 0.76 mm thick alumina plate (Al_2O_3) with a diameter of 78 mm. A 3×5 array of simulated heating chips were flush printed on the alumina surface, and the chip size is 6×5 mm. The range of voltages, which can be applied to each simulated chip having a 299–301 Ω resistance, is 0–140 V. The chip heat flux can be controlled with changing the voltage applied on the simulated chip. For the test plate, there are 17 calibrated T-type thermocouples, which have a diameter of 0.08 mm, on the simulated MCM surface installed for measuring the local temperatures of the simulated MCM surface. Besides, the middle layer is a 2 cm thick balsa slab, which is epoxied on the backside of the alumina plate to inhibit conductive heat losses from the chips. At the backside of the balsa slab, there is one thermocouple installed to evaluate the lateral conductive heat losses. In the lateral bakelite, there is also a thermocouple installed to evaluate the conductive heat loss. The bottom layer (i.e., the third layer), epoxied on the backside of balsa slab, is a 2 cm thick balsa slab. Fine holes are drilled through the balsa wood and the bakelite to allow the passage of chip leads and thermocouples. There are a total of 19 calibrated thermocouples installed for local temperature measurements of each of the test blocks in the present experiments.

2.3. Apparatus and instrumentation

As described in the previous subsection, the calibrated T-type thermocouples are epoxied on the specified locations for temperature measurements. Therefore, the local temperature distributions on the heated disk surface can be accurately measured. All the local temperatures can be accurately measured with a FLUKE-2640A data logger system interfaced to PC-AT based peripherals.

A d.c. power supply (model: GW GPD-6030, maximum operating ranges: 60 V/30 A) provides power to the heater for making the input power changeable. A precise digital multimeter (Model: YOKOGAWA 2502A, resolution: 1 μV on 100 mV range and 1 mΩ on 100 Ω range) is utilized to calibrate the voltage of each power supply and the thermal resistance of the heater.

As for emissivity measurement of the heated disk surface, a real-time infrared (IR) thermography system (Agema Thermovision 486) is capable of scanning the temperature distributions on the heated disk surface and is used for measuring the emissivity of the heated disk surface indirectly. There is a system controller for measur-

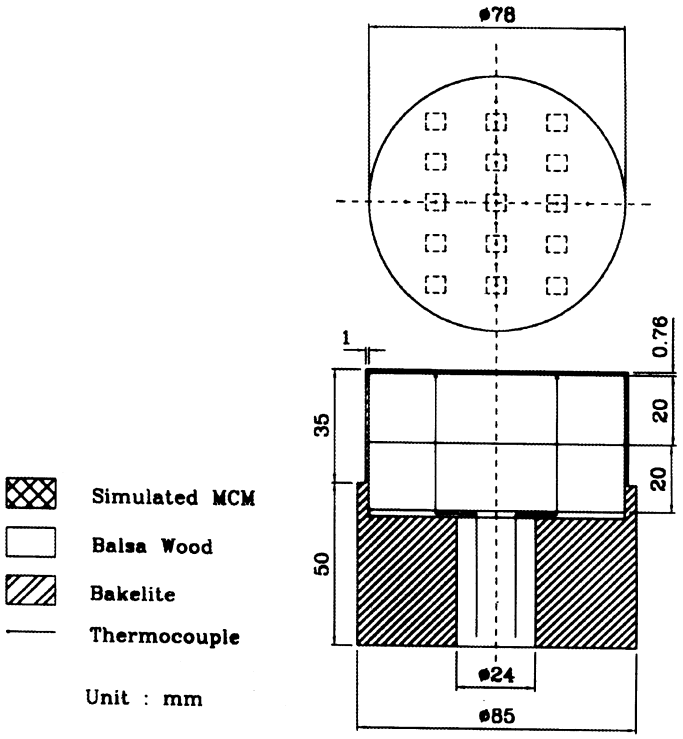

Fig. 3. Test block of heated wafer-based disk of 15 simulated multi-chip modules.

ing control and data storage. The system is equipped with a LAN interface to communicate and transfer data by way of network.

2.4. Data acquisition

The measuring system consists of a Fluke data logger and a host computer, with an Ethernet network to measure all the temperatures in the experiments. The Fluke 2640A NetDAQ networked data acquisition unit is a 20-channel front end that operates in conjunction with a PC interconnected using an Ethernet network. The usage of Ethernet network has several advantages over the traditional RS232 and IEEE-488 communication methods due to its flexibility, high data throughput and long distance between host computer and instruments.

2.5. Experimental procedure

Prior to the operation of the experiments, all the measuring instruments are calibrated, and the heated disk is positioned horizontally and installed on the rotating platform. In general, the experimental procedure includes the following steps in sequence: experimental preparations, initial temperature measurement, rotating speed setting, heater input power setting and measurement, and temperature measurement in the steady-state period.

It should be noticed that the horizontal leveling of the heated disk surface is very critical to obtain the axisymmetric temperature distribution on the heated disk surface, especially for natural convection cases. To improve measurement accuracy with calibrated T-type thermocouples, the measuring errors from different thermocouple readings for the ambient temperature prior to the operation of each experiment are eliminated.

Usually, the steady-state conditions for natural convection and rotating cases will be achieved after about 120 and 90 min from when the power is switched on, respectively.

2.6. Data reduction

The objective of the data reduction in the experiments is to get the local and average heat transfer coefficients on the heated disk surface, using an effective model to calculate the heat losses of the disk and to obtain an accurate convective heat flux.

The total steady-state heat flux generated by the chip i (i.e., $q_{t,i}$) is assumed to be composed of the following three heat-transfer modes: (1) radiative heat flux loss from chip i to the surroundings, $q_{r,i}$; (2) conductive heat flux loss to the insulated balsa wood, $q_{k,i}$; (3) convective heat flux dissipated from the chip i, $q_{c,i}$. That is

$$q_{c,i} = q_{t,i} - q_{r,i} - q_{k,i}. \tag{1}$$

Note that all the above-mentioned heat fluxes are based on chip area.

This energy-balance equation calculates the net convective heat flux, $q_{c,i}$, from the chip i to the ambient air. The total heat flux input to the simulated chip i is $q_{t,i}$ and it equals V_i^2/A_iR_i, where V_i is the output voltage of the d.c. power supply, A_i is the area of chip i, and R_i is the resistance of the chip i. Note that the heat losses through the lead wires and thermocouples are small and are neglected in the experiments. $q_{r,i}$ is evaluated with thermal diffuse gray-body networks. In the present study, the emissivity of the heated alumina disk surface is measured by an IR thermography system. $q_{k,i}$ is evaluated by a two-dimensional conduction model. The model assumes that all the conductive heat loss to the balsa wood is uniformly distributed across the surface of the heated disk, not just across the surfaces of 15 simulated chips. This assumption is very reasonable because a strong heat conduction in radial direction within the heated ceramic disk exists due to the high thermal conductivity of alumina (Al_2O_3, $k = 18$–20 W/m K) [23, 24].

To check the experimental repeatability, three sets of data were taken under the same experimental conditions for each case. The maximum deviation is less than 2.54% in the present study.

The local Nusselt number in the present study can be defined as

$$Nu_i = \frac{h_i D_h}{k_f} = \frac{q_{c,i} D_h}{(T_{w,i} - T_a)k_f} \tag{2}$$

where D_h is hydraulic diameter of simulated chips; i.e., $D_h = (2\ell w)/\ell + w)$. $T_{w,i}$ and T_a represent the local wall temperature on discrete chip i and ambient air temperature, respectively. $q_{c,i}$ is the local convective heat flux of discrete chip i.

The average Nusselt number is evaluated by the step similar to local Nusselt number, but with the difference that all the parameters are based on the whole surface, not on the heated chips. Therefore the heat flux of the test section surface is

$$q_c = q_t - q_r - q_k \tag{3}$$

where the q_t, q_r and q_k are on the basis of the whole surface area of the heated circular disk.

Thus, the average heat transfer coefficient of the heated disk can be evaluated as

$$\bar{h} = \frac{q_c}{\overline{T_w} - T_a} \tag{4}$$

and the average Nusselt number can be obtained by the following formula:

$$\overline{Nu} = \frac{\bar{h} D}{k_f} \tag{5}$$

where D is the diameter of the heated disk.

2.7. Uncertainty analysis

Using the standard single-sample uncertainty analysis recommended by Kline and McClintock [25] and Moffatt [26], the maximum uncertainties in heat flux based on the surface of the disk, heat flux based on the area of the chip, local Nusselt number, average Nusselt number, rotational Reynolds number and Grashof number are 2.25, 0.15, 2.46, 3.09, 6.96 and 2.35%, respectively.

3. Results and discussion

In this study, the main emphasis of the experimental results is on the heat transfer characteristics between a heated disk and unobstructed ambient air for both a stationary and a rotating disk. The parameters of interest in the study are the Grashof number (Gr), rotational Reynolds number (Re_r), convective chip heat flux ($q_{c,i}$). The ranges of relevant parameters studied are $Re_r = 0$–2809.5; $Gr = 4.88\times10^5$–1.92×10^6; $q_{c,i} = 1057.37$–4647.19 W/m^2, diameter of disk = 78 mm, chip size = 5×6 mm^2. In addition, the surface temperature distributions of simulated chips are precisely measured with calibrated T-type thermocouples, and they ranged between 35 and 74°C. The ambient temperatures in the experiments are varied between 24 and 32°C.

As mentioned in the previous subsection of Experimental procedure, the steady-state conditions for natural convection and rotating cases will be achieved about 120 and 90 min after the power is switched on, respectively. In the present study, two cases such as $q_{c,i} = 3387.67$ W/m^2 for natural convection and $Re_r = 265.16$ and $q_{c,i} = 3914.91$ W/m^2 for rotation heat transfer are chosen as test cases for determining the time required to achieve steady state. The results demonstrate that the maximum relative variation of average Nusselt number between 120–240 min is less than 1%, so the experimental period for all the cases in the present study is at least 180 min to ensure steady state.

3.1. Natural convection from a horizontal wafer-based disk having 15 simulated heating chips

Results of natural convection from a horizontal circular disk having 15 simulated heating chips, including the temperature distribution on the heated wafer-based disk surface and local and average heat transfer characteristics, are presented and discussed in this section.

(A) Temperature distribution on heated disk surface: the temperature distributions on the horizontal circular disk having 15 simulated heating chips are investigated for various convective heat fluxes. Since the circular disk is installed horizontally, an axisymmetric temperature distribution on the heated disk surface is expected ideally. To verify that the experimental conditions are axisymmetrically maintained and results are achieved in an axisymmetric form, all the temperatures for the simulated chips are explored. The present results reveal the axisymmetric bell-shaped profile of radial chip temperature distributions for a specified convective heat flux. Furthermore, it is also found that the chip temperature decays along the radial direction. This result may be explained from flow visualization conducted in the present study. As displayed in Fig. 4, air is drawn from the edges of the heated disk and then moves away from the heated disk surface owing to the upward buoyancy, so the cold ambient air is entrained at the region near the rim of the heated disk. Consequently, the effect of this cold ambient air on chip temperature will be significant in the region near the rim of the heated disk, and the effect will become insignificant in the region near the disk center. Therefore, the minimum chip temperature exists near the disk rim and the chip temperature increases along the distance from the disk rim toward the center.

A dimensionless temperature excess ratio is defined as the ratio of temperature excess for chip i, $T_{w,i}-T_a$, to that for average surface temperature, $\overline{T_w}-T_a$. Although the effect of convective heat flux on $(T_{w,i}-T_a)/(\overline{T_w}-T_a)$ for $q_{c,i} = 1610.27$–3910.34 W/m^2 is not significant, the actual chip temperatures on the heated disk generally increase with increasing convective heat flux at any specified radial location in the present study.

Furthermore, it should be noticed that the effect of convective heat flux or Grashof number on the distribution of $(T_{w,i}-T_a)/(\overline{T_w}-T_a)$ is not significant. That means, the distributions of $(T_{w,i}-T_a)/(\overline{T_w}-T_a)$ for various convective heat fluxes or Grashof numbers can be expressed as a generalized bell-shaped profile, which is independent of convective heat flux or Grashof number.

(B) Chip heat transfer characteristics: Fig. 5 displays the distribution of local chip Nusselt number on the heated disk surface for the cases with various Grashof numbers. The results show the axisymmetric Nu distribution achieved in the present experiments; the highest heat transfer occurs for the chip near the rim of the heated disk. The local chip Nusselt number for a specified Grashof number decreases along the distance from the disk rim toward the center as mentioned in Subsection (A). Similar trends can be found for other Grashof numbers. These results are consistent with those reported by Robinson and Liburdy [27].

Furthermore, as expected, the chip Nusselt number on the heated disk surface increases with increasing Grashof number at a specified chip on the disk surface.

(C) Average heat transfer characteristics on disk surface: the effects of average temperature excess ($\Delta\bar{T}$) and the corresponding Grashof number (Gr) on the average Nusselt number ($\overline{Nu_n}$) are shown in Fig. 6(a) and (b), respectively. Some existing correlations of natural convec-

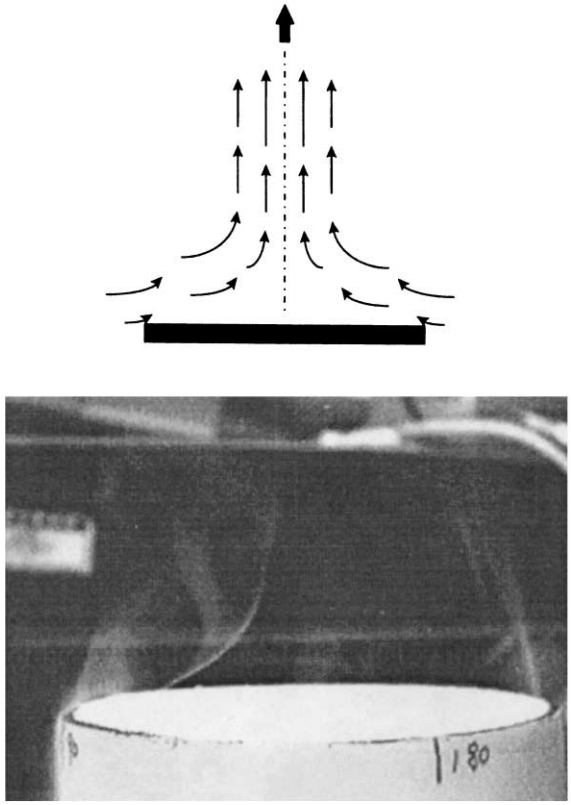

Fig. 4. Flow visualization for natural convection above the horizontal heated wafer-based disk surface.

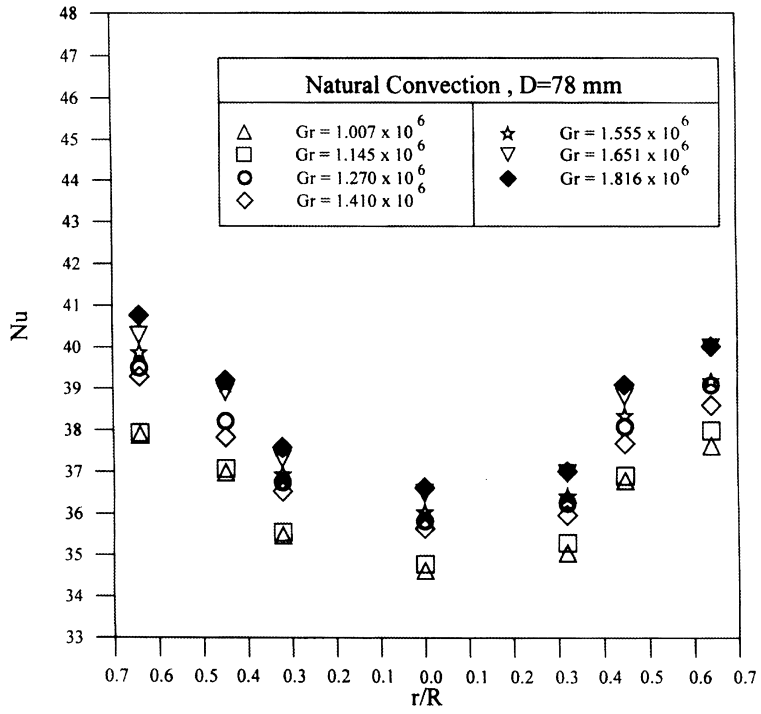

Fig. 5. Distribution of chip Nusselt numbers on heated disk surface in natural convection.

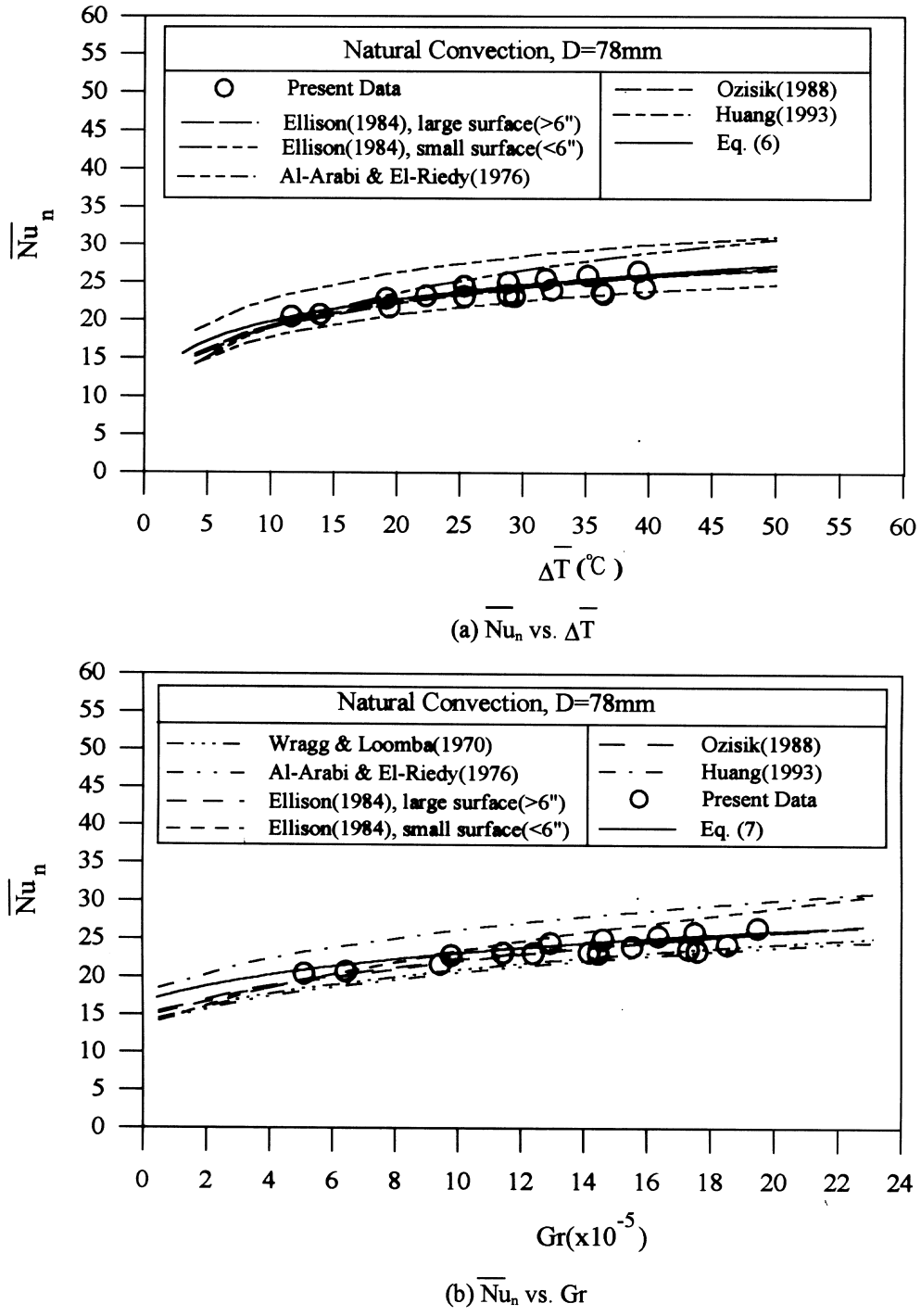

Fig. 6. Average Nusselt number on heated wafer-based disk surface.

tion form a horizontal heated disk with a finite diameter presented by the previous researchers [7–10, 28] are also plotted in the figures for comparisons. As shown in the figures, the present results are consistent with the data predicted by the above-mentioned correlations. Besides, as expected, the average Nusselt number increases with

increasing Grashof number (or average temperature excess). The relationship between $\overline{Nu}_n$ and $\Delta\bar{T}$ (or Gr) in the present data can be correlated as

$$\overline{Nu}_n = 12.118\Delta\bar{T}^{0.214} \quad (6)$$

or

$$\overline{Nu}_n = 1.455Gr^{0.2}. \quad (7)$$

The average deviations of the experimental data from the data predicted by equations (6) and (7) are 3.24 and 2.67%, respectively.

3.2. Heat transfer from a horizontal rotating wafer-based disk having 15 simulated heating chips

The temperature distribution on the heated disk surface and the local and average heat transfer characteristics from a horizontal rotating disk having 15 simulated heating chips are presented and discussed in the following sections.

(A) Temperature distribution on the heated rotating disk: the temperature distributions on the horizontal rotating disk having 15 simulated heating chips are determined for various rotational Reynolds numbers. Since the circular disk is installed horizontally and rotated with a constant revolutions per minute (rpm), an axisymmetric temperature distribution on the heated disk surface may be expected ideally. To verify that the experimental conditions are axisymmetrically maintained and the results are achieved in an axisymmetric form, all the temperatures for simulated chips are measured. Also, it is found that the chip temperature decays along the radial direction. This result may be caused by the edge effects of a disk of finite radius, e.g., flow turns, additional heat losses, etc. Therefore, the minimum chip temperature exists near the disk rim and the chip temperature increases along the distance from the disk rim toward the center. Besides, the actual chip temperature at any specified radial location on the heated disk surface generally decreases with increasing rotational Reynolds number in the present study.

Similar to the conclusion made for natural convection from a horizontal circular heated disk, the effect of rotational Reynolds number, instead of Grashof number in natural convection, on the distribution of $(T_{w,i}-T_a)/(\overline{T}_w-T_a)$ is not significant. That means, the distributions of $(T_{w,i}-T_a)/(\overline{T}_w-T_a)$ for various rotational Reynolds numbers can be expressed as a generalized bell-shaped profile, which is independent of rotational Reynolds number.

(B) Chip heat transfer characteristics: the distributions of chip Nusselt numbers on the heated wafer-based disk surface for the cases with various rotational Reynolds numbers under different Grashof numbers are displayed in Fig. 7(a) and (b). The results reveal that the axisymmetric bowl-shaped Nu distribution is achieved in the present experiments; and the highest heat transfer occurs for the chip near the rim of the heated disk. Besides, the local chip Nusselt number for specified rotational Reynolds number and Grashof number increases along the distance from the disk center toward the rim. This result may be due to the edge effects of a disk of finite radius, e.g., flow turns, additional heat losses, etc. Therefore, the maximum chip heat transfer performance exists near the disk rim and the chip heat transfer performance decreases along the distance from the disk rim toward the center. Additionally, the chip Nusselt number at any specified chip on the heated disk surface generally increases with increasing rotational Reynolds number in the present study.

(C) Average heat transfer characteristics on disk surface: the relationship of average Nusselt number in terms of rotational Reynolds number and Grashof number is shown in Fig. 8. From the figure, the average Nusselt number increases with increasing rotational Reynolds number at a specified Grashof number. Besides, the effect of Grashof number on average Nusselt number will become more significant when the rotational Reynolds number decreases; while it will become insignificant when $Re_r \geqslant 1112$. This means, the average Nusselt number at high rotational Reynolds number is a function of rotational Reynolds number only. This conclusion can be verified by the laminar Nusselt correlations presented by Kreith [29] and Cobb and Saunders [30]. Their correlations for an isothermal disk rotating in still air can be respectively expressed as

$$\overline{Nu}_r = 0.66Re_r^{1/2} \quad [29] \quad (8)$$

and

$$\overline{Nu}_r = 0.72Re_r^{1/2} \quad [30]. \quad (9)$$

Equations (8) and (9) are also plotted in Fig. 8 for comparisons. When the rotational Reynolds number increases, the present experimental data for various convective heat fluxes will approach the Cobb and Saunders' correlation. A significant deviation of the present experimental data from the results evaluated by equation (8) or (9) will be found when the rotational Reynolds number decreases. In other words, the buoyancy effect on heat transfer characteristics of the rotating disk will become more significant; consequently, the strength of mixed convection will increase when the rotational Reynolds number decreases.

3.2.1. Composite correlation for mixed convection due to mutual effect of rotation and buoyancy

Based on the results shown in Fig. 8, it is interesting to point out that mixed convection will dominate the heat transfer behavior of the heated rotating disk at the condition with both a low/moderate rotational Reynolds

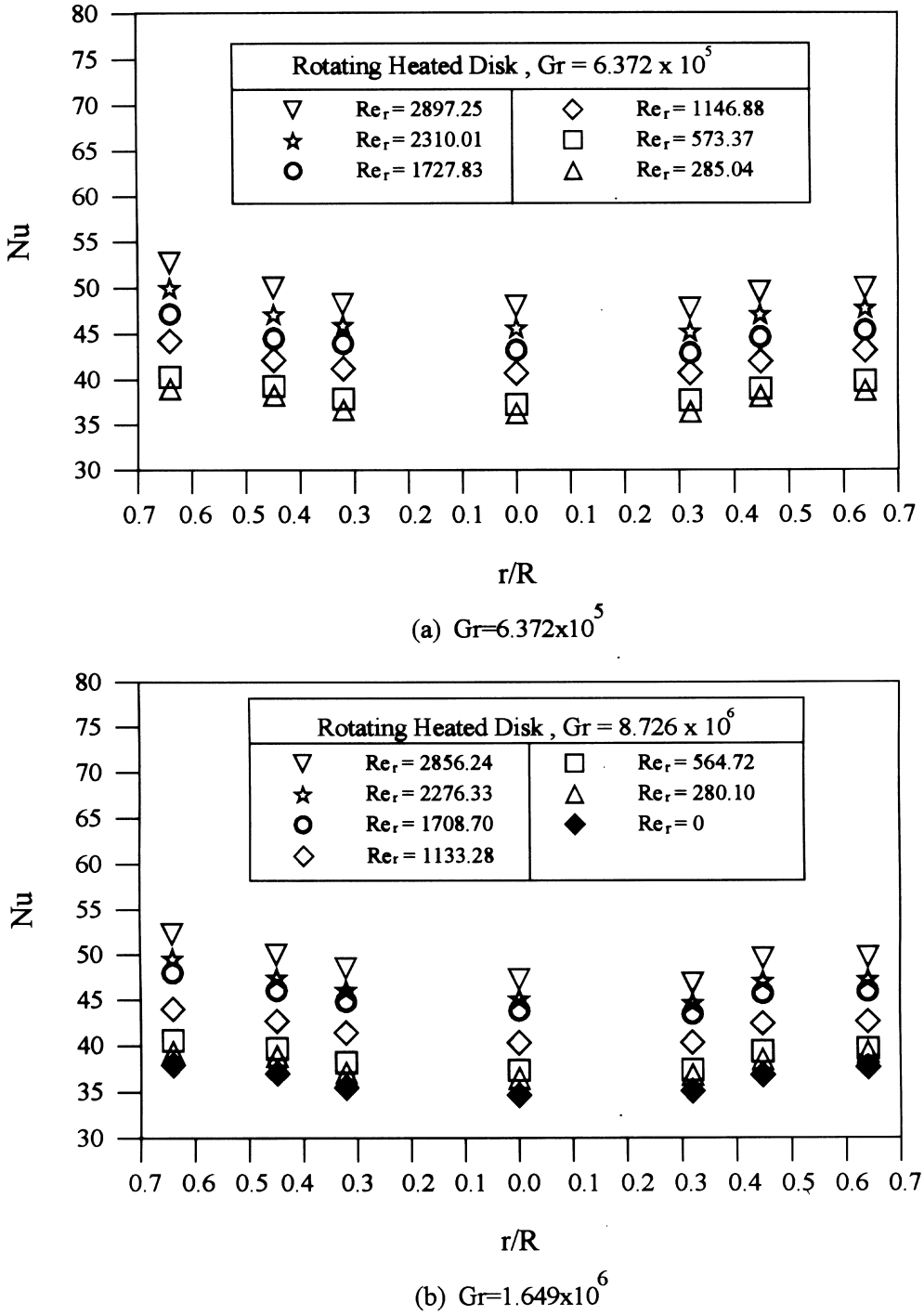

Fig. 7. Distributions of chip Nusselt numbers on rotating heated disk for various rotational Reynolds numbers.

number and a high Grashof number. In order to interpret and predict the average Nusselt number from buoyancy-dominated regime to rotation-dominated regime, it is very important to postulate a new composite correlation for dealing with this kind of problem.

According to the method presented by Churchill and

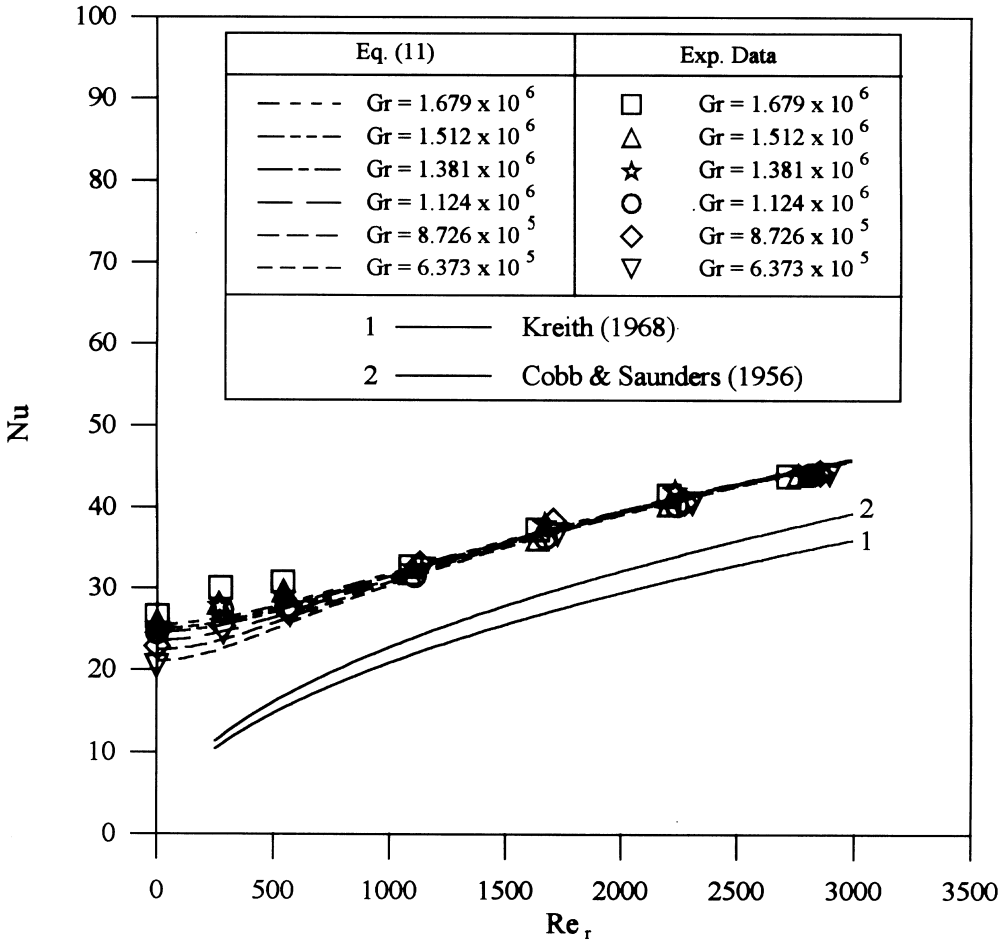

Fig. 8. Effect of rotational Reynolds number on average Nusselt number of rotating heated disk.

Usagi [31], a composite correlation of average Nusselt number can be constructed based on the average Nusselt numbers in natural convection, $\overline{Nu}_n$, and in purely forced convection of rotation, $\overline{Nu}_r$, in the following form:

$$\overline{Nu}^n = \overline{Nu}_r^n + \overline{Nu}_n^n. \tag{10}$$

In equation (10), $\overline{Nu}_n$ can be evaluated by equation (7); $\overline{Nu}$ which includes the effects of rotation and buoyancy is determined in the present study. With the two limiting conditions (i.e., purely natural convection and purely forced convection of rotation) and curve fitting of the experimental data by a least squares method, a new composite correlation of average Nusselt number for mixed convection due to rotation and buoyancy is

$$\overline{Nu}^5 = \overline{Nu}_r^5 + \overline{Nu}_n^5 \tag{11}$$

where

$$\overline{Nu}_r = 1.855 Re_r^{0.4} \tag{12}$$

and

$$\overline{Nu}_n = 1.455 Gr^{0.2}. \tag{7}$$

Comparisons of the predictions evaluated by equation (11) with the present experimental data are made and shown in Fig. 9. The average deviation between them is 3.14%.

3.2.2. Heat transfer regimes

In order to further examine the effects of rotation and buoyancy on average Nusselt number, equation (11) can be rewritten and expressed in the following two forms:

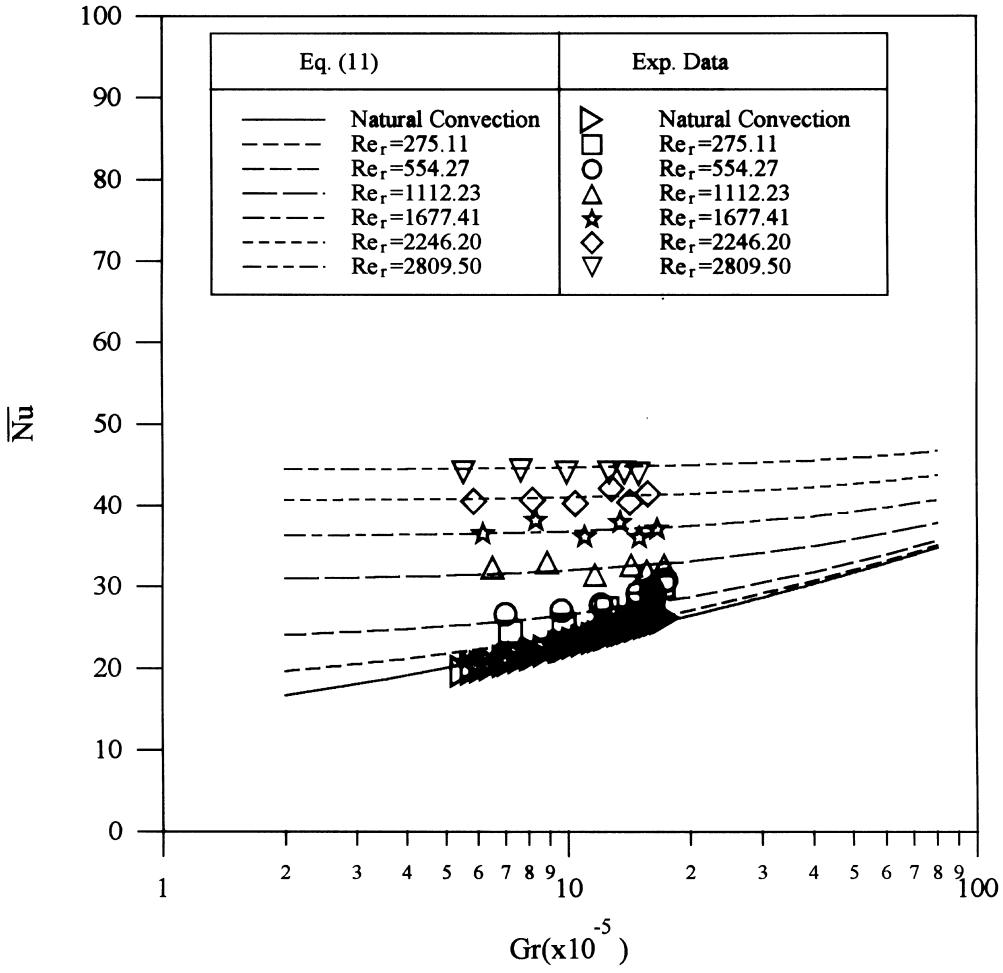

Fig. 9. Comparison of predicted $\overline{Nu}$ results with experimental data.

$$\frac{\overline{Nu}}{\overline{Nu}_n} = \left[1 + 3.368\left(\frac{Gr}{Re_r^2}\right)^{-1}\right]^{1/5} \tag{13}$$

and

$$\frac{\overline{Nu}}{\overline{Nu}_r} = \left[1 + 0.297\left(\frac{Gr}{Re_r^2}\right)\right]^{1/5}. \tag{14}$$

Equations (13) and (14) are plotted and shown in Fig. 10(a) and (b), respectively. The effects of rotation and buoyancy on the average Nusselt numbers are significant when $\overline{Nu}/\overline{Nu}_n > 1.05$ or $\overline{Nu}/\overline{Nu}_r > 1.05$, respectively. In the present experiments, the ranges of Gr/Re_r^2 representing the regimes of significant rotation effect and of significant buoyancy effect are determined as:

(a) when $Gr/Re_r^2 < 12.191$ (at $\overline{Nu}/\overline{Nu}_n > 1.05$): significant rotation effect;
(b) when $Gr/Re_r^2 > 0.931$ (at $\overline{Nu}/\overline{Nu}_n > 1.05$): significant buoyancy effect.

As shown in Fig. 11, based on the present experimental data and the above discussion, three heat transfer regimes in the present study can be concluded as follows:

Regime (I) Dominated by purely forced convection of rotation: $Gr/Re_r^2 \leqslant 0.931$;
Regime (II) Dominated by mixed convection: $0.931 < Gr/Re_r^2 < 12.191$;
Regime (III) Dominated by purely natural convection: $Gr/Re_r^2 \geqslant 12.191$.

3.2.3. *New explicit form of composite* $\overline{\mathrm{Nu}}$ *correlation*

To interpret the relative influence of buoyancy to rotation in the present mixed convection problems, another new explicit form of composite $\overline{Nu}$ correlation in terms of a unique parameter of Gr_r^2, instead of the form presented by equation (11) which is in terms of Gr and Re_r, is more meaningful and valuable to be proposed in

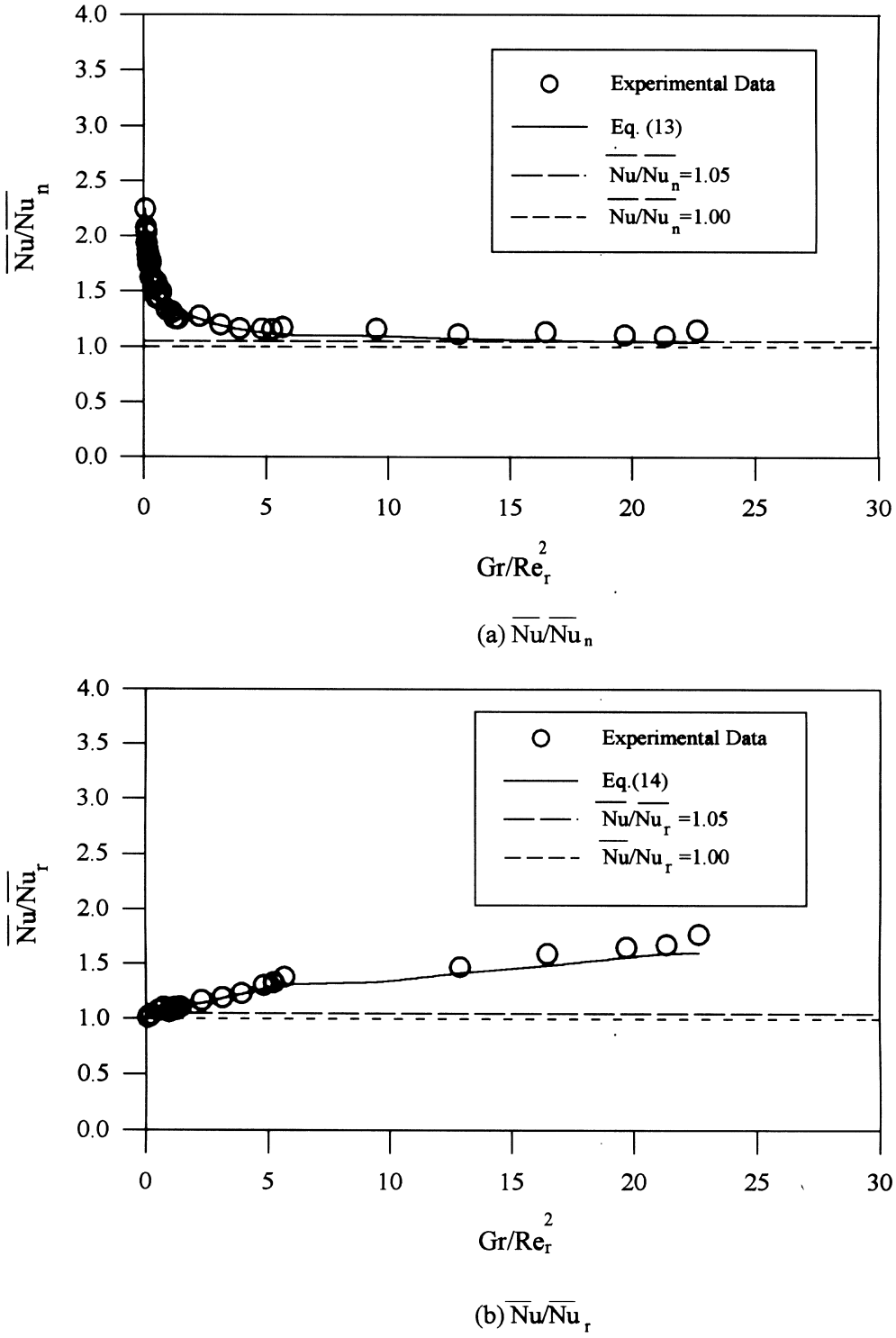

Fig. 10. Effects of rotation and buoyancy on average Nusselt number.

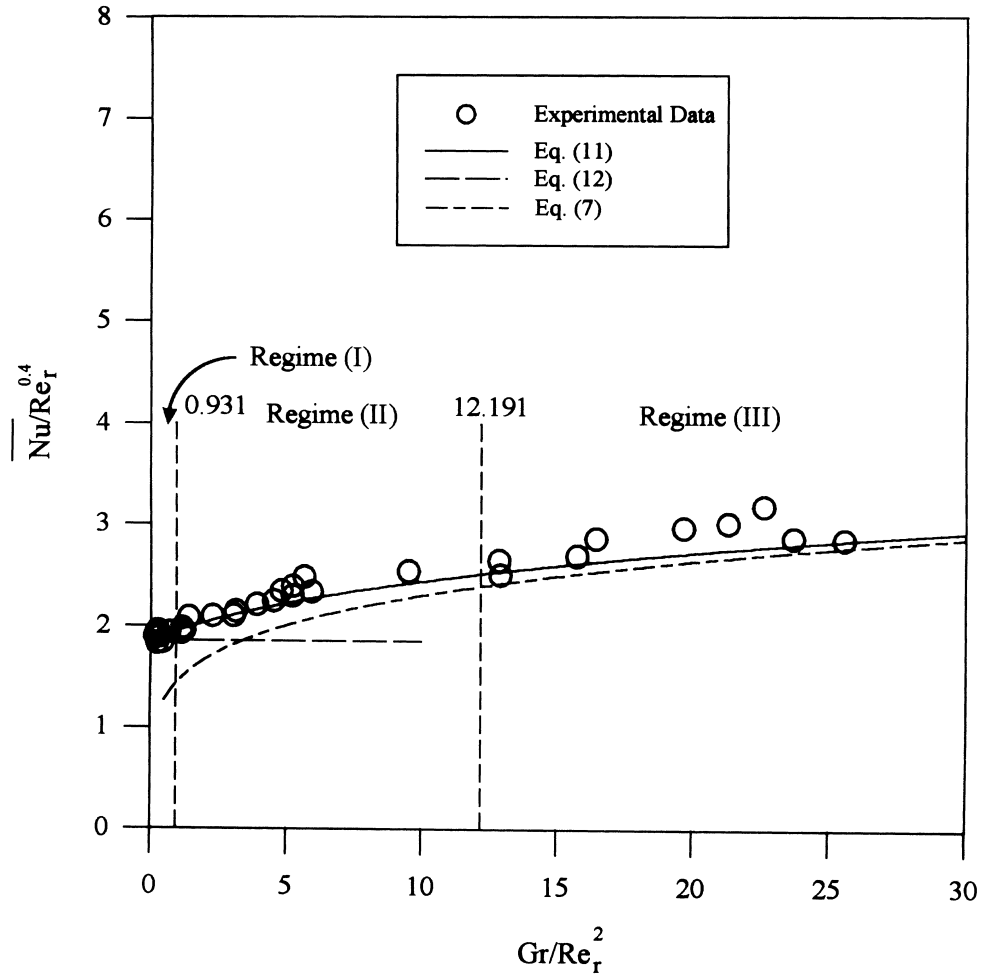

Fig. 11. Heat transfer regimes for horizontal heated wafer-based disk under the mutual effect of rotation and buoyancy.

the present study. The modified explicit correlation based on Gr/Re_r^2 can be expressed in the following form:

$$\overline{Nu} = \left[2.718\times10^{7}\left(\frac{Gr}{Re_r^2}\right)^{-1} + 7.518\times10^{5}\left(\frac{Gr}{Re_r^2}\right)\right]^{1/5}. \tag{15}$$

The range of parametric validity for using equation (15) in the present study is $0.0657 \leqslant Gr/Re_r^2 \leqslant 25.579$. Comparisons of the predictions evaluated by equation (15) with the present experimental data are made and shown in Fig. 12. The average deviation between them is 7.03%.

4. Concluding remarks

The main conclusions emerging from the results and discussion may be summarized as follows:

(1) An experimental model for the analysis of heat transfer characteristics of a heated disk at rest and in rotation has been successfully established in the present research.
(2) With this analysis, the evaluation of heat transfer characteristics of natural convection from a horizontal heated disk are quite consistent with those presented in the existing literature.
(3) In both the stationary and the rotating cases, it is found that an axi-symmetric bowl-shaped *Nu* profile is obtained. The local Nusselt number, for specified rotational Reynolds number and Grashof number, decreases along the distance from the disk rim toward the center i.e., the highest heat transfer performance occurs at the chip near the rim of the heated disk. Additionally, the chip Nusselt number at any specified chip on the heated disk surface generally increases with increasing Grashof number or rotational Reynolds number.

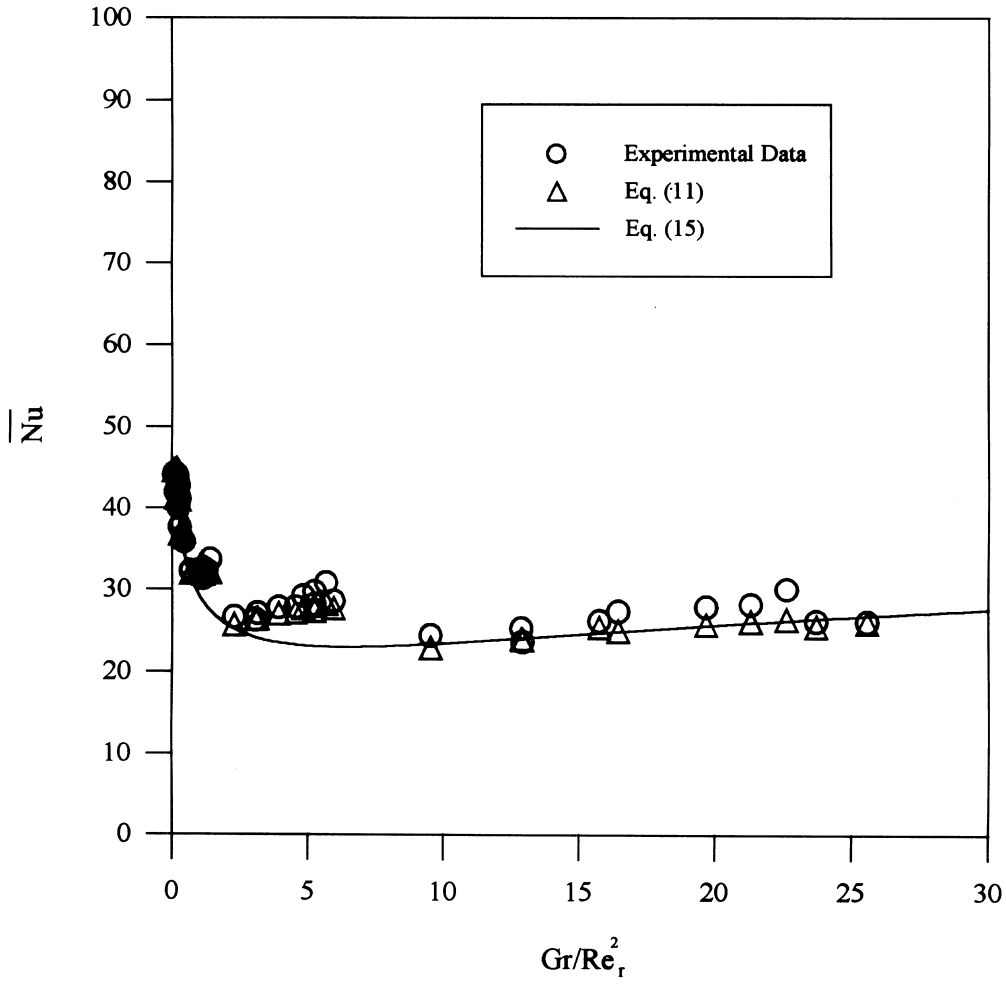

Fig. 12. Comparisons between the proposed explicit $\overline{Nu}$ correlation and experimental data.

(4) The average Nusselt number increases with increasing rotational Reynolds number and Grashof number. However, the contribution of Grashof number to average Nusselt number will become more significant when the rotational Reynolds number is small; in the studied range of Grashof number, will become insignificant when $Re_r \geqslant 1112$.
(5) The heat transfer behaviors for a horizontal heated wafer-based disk caused by the mutual effect between disk rotation and buoyancy can be classified into three heat transfer regimes: (a) purely forced convection of rotation, (b) mixed convection and (c) purely natural convection.
(6) The new implicit and explicit composite correlations of average Nusselt number for mixed convection due to rotation and buoyancy are proposed. By comparing the predictions evaluated by these two correlations with the present experimental data, it is found that average deviations are 3.14 and 7.03%, respectively.

Acknowledgement

The authors wish to thank the support of the National Science Council, Taiwan, Republic of China under grant No. NSC82-0404-E-007-135.

References

[1] A.E. Bergles, Evolution of cooling technology for electrical, electronic, and microelectronic equipment, in: Heat Transfer in Electronic Equipment—1986, ASME, New York, 1986, pp. 1–9.
[2] C. Yih, Free convection due to a point source of heat,

Proceedings of the 1st National Congress of Applied Mechanics, 1951, pp. 941–947.
[3] T. Fujii, Theory of the steady laminar natural convection above a horizontal line heat source on a point heat source, Int. J. Heat Mass Transfer 6 (1963) 597–606.
[4] Z. Rotem, L. Claassen, Natural convection above unconfined horizontal surfaces, J. Fluid Mechanics 9 (1969) 173–192.
[5] R.J. Goldstein, E.M. Sparrow, D.C. Jones, Natural convection mass transfer adjacent to horizontal plates, Int. J. Heat Mass Transfer 16 (1973) 1025–1035.
[6] R.J. Goldstein, K.S. Lau, Laminar natural convection from a horizontal plate and the influence of plate-edge extensions, J. Fluid Mech. 129 (1983) 55–75.
[7] M. Al-Arabi, M.K. El-Riedy, Natural convection heat transfer from isothermal horizontal plates of different shapes, Int. J. Heat Mass Transfer 19 (1976) 1399–1404.
[8] G.N. Ellison, Thermal Computations for Electronic Equipment, Van Nostrand Reinhold Co., New York, 1984.
[9] M.N. Ozisik, Y. Bayazitoglu, Elements of Heat Transfer, McGraw-Hill, New York, 1988.
[10] C.L. Huang, Heat transfer characteristics of a confined round jet impingement, Master's Thesis, Department of Power Mechanical Engineering, National Tsing Hua University, Taiwan, 1993.
[11] T. von Karman, On laminar and turbulent friction, NACA Report No. 1902, 1946.
[12] C. Wanger, Heat transfer from a rotating disk to ambient air, J. Appl. Phys. 19 (1948) 837–839.
[13] J.P. Hartnett, Heat transfer from a nonisothermal disk rotating in still air, J. Appl. Mech. 26 (1959) 672–673.
[14] E.M. Sparrow, J.L. Gregg, Heat transfer from a rotating disc to fluids of any Prandtl number, ASME J. Heat Transfer 81 (1959) 249–251.
[15] N. Riley, The heat transfer from a rotating disk, Quart. J. Mech. App. Math. 17 (1964) 331–349.
[16] F. Kreith, J.H. Taylor, J.P. Chong, Heat transfer and mass transfer from a rotating disk, ASME J. Heat Transfer 81 (1959) 95–105.
[17] C.L. Tien, Heat transfer by laminar flow from a rotating cone, ASME J. Heat Transfer 82 (1960) 252–253.
[18] S. Screenivasan, Laminar mixed convection from a rotating disc, Int. J. Heat Mass Transfer 16 (1973) 1489–1492.
[19] C.O. Popie, L. Boguslawski, Local heat-transfer coefficients on the rotating disk in still air, Int. J. Heat Mass Transfer 18 (1975) 167–170.
[20] D.L. Oehlbeck, F.F. Erian, Heat transfer from axisymmetric sources at the surface of a rotating disk, Int. J. Heat Mass Transfer 22 (1979) 601–610.
[21] H.T. Lin, L.K. Lin, Heat transfer from a rotating cone or disk to fluids of any Prandtl number, Int. Comm. Heat Mass Transfer 14 (1987) 323–332.
[22] J.M. Owen, R.H. Rogers, Flow and Heat Transfer in Rotating Disc Systems, Vol. 1—Rotor-Stator Systems, Research Studies Press, Taunton, U.K., 1989.
[23] F.P. Incropera, D.P. Dewitt, Fundamentals of Heat and Mass Transfer, 2nd ed., Purdue University, IN, 1985, pp. 755–757.
[24] R.R. Tummala, E.J. Rymaszewski, (Eds), Microelectronics Packaging Handbook, Van Nostrand Reinhold, New York, 1989, p. 36.
[25] S.J. Kline, F.A. McClintock, Describing uncertainties in single-sample experiments. Mech. Engng 3–8 (Jan. 1953).
[26] R.J. Moffat, Describing the uncertainties in experimental results, Expl. Thermal Fluid Sci. 1 (1988) 3–17.
[27] S.B. Robinson, J.A. Liburdy, Prediction of the natural convective heat transfer from a horizontal heated disk, ASME J. Heat Transfer 109 (1987) 906–911.
[28] A.A. Wragg, R.P. Loomba, Free convection flow patterns at horizontal surfaces with ionic transfer, Int. J. Heat Mass Transfer 13 (1970) 439–442.
[29] F. Kreith, Convection heat transfer in rotating systems, Advances in Heat Transfer 5 (1968) 129–251.
[30] E.C. Cobb, O.A. Saunders, Heat transfer from a rotating disk, Proc. Roy. Soc. A 236 (1956) 343–351.
[31] S.W. Churchill, R. Usagi, A general expression for the correlation of rates of transfer and other phenomena, AIChE Journal 18 (1972) 1121–1128.